Salusin-α alleviates lipid metabolism disorders via regulation of the downstream lipogenesis genes through the LKB1/AMPK pathway

JINTONG PAN[1*], CHAO YANG[1,2*], AOHONG XU[1], HUAN ZHANG[1], YE FAN[1], RONG ZENG[1,2], LIN CHEN[1,2], XIANG LIU[1,2] and YUXUE WANG[1,2]

[1]Department of Laboratory Medicine, Hubei University of Chinese Medicine, Wuhan, Hubei 430065, P.R. China; [2]Hubei Shizhen Laboratory, Hubei University of Chinese Medicine, Wuhan, Hubei 430065, P.R. China

Received January 24, 2024; Accepted June 5, 2024

DOI: 10.3892/ijmm.2024.5397

Abstract. Lipid metabolism disorders are a major cause of several chronic metabolic diseases which seriously affect public health. Salusin-α, a vasoactive peptide, has been shown to attenuate lipid metabolism disorders, although its mechanism of action has not been reported. To investigate the effects and potential mechanisms of Salusin-α on lipid metabolism, Salusin-α was overexpressed or knocked down using lentiviral vectors. Hepatocyte steatosis was induced by free fatty acid (FFA) after lentiviral transfection into HepG2 cells. The degree of lipid accumulation was assessed using Oil Red O staining and by measuring several biochemical indices. Subsequently, bioinformatics was used to analyze the signaling pathways that may have been involved in lipid metabolism disorders. Finally, semi-quantitative PCR and western blotting were used to verify the involvement of the liver kinase B1 (LKB1)/AMPK pathway. Compound C, an inhibitor of AMPK, was used to confirm this mechanism's involvement further. The results showed that Salusin-α significantly attenuated lipid accumulation, inflammation and oxidative stress. In addition, Salusin-α increased the levels of LKB1 and AMPK, which inhibited the expression of sterol regulatory element binding protein-1c, fatty acid synthase and acetyl-CoA carboxylase. The addition of Compound C abrogated the Salusin-α-mediated regulation of AMPK on downstream signaling molecules. In summary, overexpression of Salusin-α activated the LKB1/AMPK pathway, which in turn inhibited lipid accumulation in HepG2 cells. This provides insights into the potential mechanism underlying the mechanism by which Salusin-α ameliorates lipid metabolism disorders while identifying a potential therapeutic target.

Correspondence to: Dr Xiang Liu or Dr Yuxue Wang, Department of Laboratory Medicine, Hubei University of Chinese Medicine, 16 Huangjiahu West Road, Wuhan, Hubei 430065, P.R. China
E-mail: lx1568@hbtcm.edu.cn
E-mail: wangyuxue@hbtcm.edu.cn

*Contributed equally

Abbreviations: FFA, free fatty acid; LKB1, liver kinase B1; AMPK, adenosine 5'-monophosphate (AMP)-activated protein kinase; SREBP-1c, sterol regulatory element binding protein-1c; FASN, fatty acid synthase; ACC, acetyl-CoA carboxylase; NAFLD, non-alcoholic fatty liver disease; TG, triglycerides; ALT, alanine aminotransferase; AST, aspartate aminotransferase; MDA, malondialdehyde; SOD, superoxide dismutase

Key words: salusin-α, lipid metabolism disorders, LKB1, AMPK, SREBP-1c, HepG2

Introduction

Lipid metabolism disorders refer to the abnormal changes in lipids and their metabolites in the blood and other tissues and organs, resulting from congenital or acquired factors. Such disorders are associated with the development of various diseases, including diabetes, hyperlipidemia, atherosclerosis, and even certain neurodegenerative diseases and tumors (1,2). Non-alcoholic fatty liver disease (NAFLD) is a clinical syndrome in which the diffuse bulla fat of hepatocytes exhibits excessive accumulation of lipids in hepatocytes but excludes liver pathologies caused by excessive alcohol consumption and other definitive liver damage factors. The prevalence of NAFLD is increasing annually, as is the trend of incidence in younger individuals (3,4). However, there are currently no FDA-approved drugs available to treat NAFLD. Given the critical role of lipid metabolism disorders in the occurrence and development of NAFLD (5,6), it is important to explore methods to alleviate lipid metabolism disorders of the hepatocytes in patients with fatty liver disease to reduce the incidence of NAFLD (7,8).

Salusin-α, one of the products of selective splicing of the dystonia-associated gene (TOR2A), is a biologically active peptide consisting of 28 amino acid residues with hemodynamic and mitogenic activity (9). It is widely found in tissues and the body fluids of humans, rats and mice, such as in the vascular endothelium, kidneys, brain, plasma, urine and other secretions (10-12). Previous studies have demonstrated that Salusin-α can reduce lipid accumulation and is associated

with improved lipid profiles, which inhibit coronary artery disease (13-15). Animal experiments have shown that Salusin-α can also inhibit liver steatosis and reduce plasma TG levels in mice (16). The authors' research group previously established a new method of targeting the delivery of EGFP-Salusin-α plasmid to the arterial endothelia and demonstrated that Salusin-α can reduce atherosclerosis in rabbits (17), and it was also demonstrated that Salusin-α may inhibit hepatocyte lipid synthesis through the PPARα/ApoA5/sterol regulatory element binding protein-1c (SREBP-1c) pathway (18). Nevertheless, the exact mechanism by which Salusin-α affects hepatocyte lipid metabolism remains incompletely understood. Exploring the potential mechanism of the regulation of Salusin-α for lipid metabolism in hepatocytes may provide a potential target for NAFLD treatment.

Accordingly, in the present study, the related factors and signaling pathways by which Salusin-α may exert its effects on lipid metabolism in hepatocytes were assessed using lentiviral vectors to overexpress or knockdown Salusin-α expression into HepG2 cells and then inducing their steatosis. This model provides a practical basis for studying the potential mechanism of Salusin-α to prevent lipid metabolism disorders and provides a potential target for the treatment of NAFLD.

Materials and methods

Lentivirus packaging and establishment of hepatocyte steatosis model

Cell culture and lentivirus packaging. HepG2 and 293T cells were purchased from SUNNCELL (sunncell.com.cn; cat. nos. SNL-083 and SNL-015). HepG2 is a liver cancer cell line exhibiting epithelial-like morphology that was isolated from a hepatocellular carcinoma in white male patient with liver cancer and 293T is an epithelial-like cell that was isolated from the kidney of a patient. Both cell lines were authenticated using short tandem repeat, and they matched the HepG2 (cat. no. ACC-180) and 293T (cat. no. ACC-635) cells in the DSMZ database. Both cells were cultured in DMEM high glucose medium (cat. no. PM150210; Procell Life Science & Technology Co., Ltd.) supplemented with 10% (v/v) fetal bovine serum, 100 U/ml penicillin and 100 μg/ml streptomycin (cat. no. MA0110; Dalian Meilun Biology Technology Co., Ltd.). Cells were maintained in a humidified incubator at 37˚C and supplied with 5% CO_2 air. The construction and packaging of lentiviral vectors containing the recombinant plasmids of Salusin-α overexpression and interference, including pHAGE-Salusin-α and pLKO.1-shSalusin-α, was performed as previously described (18). The sense and antisense sequences of short hairpin (sh)RNA are as follows: shSalusin-α sense, 5'-CCGGGCCCTTCCTCCCGCTCCAGCGCTCGAGCGCTGGAGCGGGAGGAAGGGCTTTTTG-3' and antisense, 5'-AATTCAAAAAGCCCTTCCTCCCGCTCCAGCGCTCGAGCGCTGGAGCGGGAGGAAGGGC-3'; and shMock, 5'-CCGGCAACAAGATGAAGAGCACCAACTCGAGTTGGTGCTCTTCATCTTGTTGTTTTTG-3' (cat. no. SHC002; Sigma-Aldrich; Merck KGaA).

Lentiviral vector titer assay and transmission electron microscopy (TEM) sample preparation. The titer of lentivirus was estimated using the antibiotic screening method. Firstly, an equal number of HepG2 cells were cultured at $2x10^5$ in a six-well plate, and 0, 5, 10, 15, 20, and 30 μl crude virus was added, followed by the addition of polybrene at a final concentration of 8 μg/ml (cat. no. BL628A; Beijing Labgic Technology Co., Ltd.). After the cell density reached 60-80%, the cells were collected and evenly divided into two plates, one with a concentration of 2 μg/ml puromycin dihydrochloride (cat. no. 1299MG025; Biofroxx; neoFroxx) and one without treatment. When all the cells in the antibiotic-treated plate had died, the two plates were stained with Trypan blue (cat. no. C0040; Beijing Solarbio Science & Technology Co., Ltd.) at 37˚C for 3 min and using a light microscope (Olympus Corporation), the live cells were counted. The antibiotic-treated plates were defined as 'viable cell counts', and the non-treated plates were defined as 'control cell counts'. The activity titer of each viral dose group was calculated as follows: titer [Infectious units (IFU)/ml=(number of live cells x number of starting cells)/(number of control cells x viral volume)], and finally, the mean value of each well was calculated, which was taken as the final titer of the virus. IFU is the ability of a virus to infect a host cell.

293T cells were cultured for 72 h, fixed with pre-cooled 2.5% glutaraldehyde (cat. no. G916054; Shanghai Macklin Biochemical Co., Ltd.) for 1 h, and then transferred to centrifuge tubes. Centrifugation was performed at 4˚C, at a speed of 500 x g for 5 min to remove most of the supernatant, and 1 ml of the supernatant was left to be gently resuspended and transferred to a 1.5 ml centrifuge tube for passive sedimentation for 1 h after which the supernatant was removed and fresh pre-cooled 2.5% glutaraldehyde was added, and then stored at 4˚C until they were sent to the Center of Ultramicropathology (People's Hospital of Wuhan University) for analysis.

Establishment of the hepatocyte steatosis model. According to a recent study by the authors (19), the free fatty acid (FFA) group used 200 μM FFAs to construct the cellular steatosis model. First, a 10 mM oleic acid (OA) stock solution (Shanghai Macklin Biochemical Co., Ltd.) was prepared by fully dissolving OA with NaOH. Next, 10% fatty acid-free bovine serum albumin (d-BSA; MilliporeSigma) was added to the OA solution. Similarly, a 20 mM palmitic acid (PA) stock solution (Shanghai Macklin Biochemical Co., Ltd.) was prepared using the same method. Both solutions were then filtered through a 0.22-μm bacterial filter for short-term storage at 4˚C in a refrigerator. For the induction of cellular steatosis, $1x10^6$ HepG2 cells/well were inoculated in six-well plates for 24 h and cultured until they reached 70% density, after which cells were washed twice with PBS and next treated with 200 μM of the prepared FFA working solution (200 μM FFA ready to use, obtained by adding 100 μl of the OA and PA stock solution to 10 ml DMEM high glucose complete medium, nOA:nPA=2:1). The treated cells were cultured for a further 24 h. For the control group, equal concentrations of solvents (10% d-BSA fully dissolved in NaOH) were used, as aforementioned.

Validation of the impact of Salusin-α on lipid metabolism in HepG2 cells

Effect of Salusin-α on FFA-induced HepG2 cells. Once the model had been successfully established, subsequent experiments were performed. First, $1x10^6$ cells/well were inoculated and cultured in a six-well plate for 24 h until

they reached 70% density. Next the overexpression pHAGE null virus, pHAGE-Salusin-α virus, shMock null virus, or pLKO.1-shSalusin-α virus was added, and 160 μl 8 μg/ml Polybrene was co-incubated at 37˚C for 15 min. Next, the media was topped up to 2 ml per well. After transfection for 24 h, 200 μM FFA was added to each well for another 24 h. The control group was left untreated.

Oil red O staining. The degree of lipoatrophy of HepG2 cells after induction was detected by oil red O staining. Cells were washed with PBS, then fixed with tissue fixative (cat. no. G1101; Wuhan Servicebio Technology Co., Ltd.) at room temperature for 25 min, and washed for 1 min with 60% isopropanol to remove the excess fixative. Oil red O stain (cat. no. O8010; Beijing Solarbio Technology Co., Ltd.) was used to detect lipoatrophy. The nuclei were counterstained with hematoxylin (cat. no. BL700B; Beijing Labgic Technology Co., Ltd.) for 2 min, and finally, the stained HepG2 cells were observed using a light microscope (Olympus Corporation). ImageJ (version 1.8.0.112; National Institutes of Health) was used to quantify the lipid droplet area.

Biochemical analysis of metabolic and oxidative stress indicators. Cell homogenates were collected separately after lysis with RIPA lysate (cat. no. MAO151; Dalian Meilun Biology Technology Co., Ltd.). The levels of triglyceride (TG), alanine aminotransferase (ALT), aspartate aminotransferase (AST), malondialdehyde (MDA) and superoxide dismutase (SOD) were measured according to the manufacturer's protocol (Nanjing Jiancheng Bioengineering Research Institute).

Bioinformatics analysis. To determine the related factors and pathway signals involved in the process of lipid accumulation of hepatocytes, the differentially expressed genes (DEGs) between healthy individuals and patients with NAFLD were determined using the GSE31803 dataset (https://www.ncbi.nlm.nih.gov/geo/query/acc.cgi?acc=GSE31803) from Gene Expression Omnibus database (https://www.ncbi.nlm.nih.gov/geo/). Next, the DEGs were analyzed using the DAVID database (https://david.ncifcrf.gov/) to identify the upregulated and downregulated genes. Gene Ontology (GO) analysis of the DEGs was performed to obtain the GO terms based on gene function and classification; similarly, Kyoto Encyclopedia of Genes and Genomes (https://www.genome.jp/kegg/) pathway enrichment analysis was performed on the DEGs. Together, the genes and pathways related to fatty acid oxidative catabolism-related factors and their signaling pathways were identified.

Validation of associated pathway factors

Semi-quantitative PCR (SQ-PCR) for analysis of the mRNA expression levels of relevant pathway factors. Total RNA was extracted from HepG2 cells using TRIzol™ lysis reagent (cat. no. 9108; Takara Bio, Inc.). Reverse transcription was then performed following the protocol of the reverse transcription kit (cat. no. D7170M; Beyotime Institute of Biotechnology). A total of 2 μl template was reverse transcribed to cDNA, and then 1.6 μl cDNA template was amplified into DNA using Taq DNA Polymerase (cat. no. ET101; Tiangen Biotech Co., Ltd.). To ensure reliable results and minimize potential variations, the optimal temperature and number of cycles for each primer were determined in the logarithmic growth phase using a control group. The primer sequences used are provided in Table I. The thermocycling conditions were as follows: Pre-denaturation of Salusin-α at 94˚C for 3 min, followed by 30 cycles of denaturation at 94˚C for 30 sec, annealing at 64˚C for 30 sec, and extension at 72˚C for 30 sec. A final extension step was performed at 72˚C for an additional 5 min. For annealing of AMPK, SREBP-1c, acetyl-CoA carboxylase (ACC), fatty acid synthase (FASN), monocyte chemoattractant protein-1 (MCP-1) and transforming growth factor β (TGF-β), a temperature of 58˚C was used for 36 cycles. In comparison, liver kinase B1 (LKB1) was annealed at 59˚C for 36 cycles, and GAPDH was annealed at 60˚C for 30 cycles. The remaining steps were consistent with those used for Salusin-α. Following amplification, the PCR products were separated on a 1.5% agarose gel electrophoresis and visualized using the Tanon 1600 Gel Imaging System (Tanon Science and Technology Co., Ltd.). To quantify the changes in the expression of each target gene, the optical density (OD) values of the bands were analyzed using the Tianneng gel analysis software (biotanon.com). The relative expression levels of each mRNA were determined by calculating the ratio of the OD value of the target gene to the OD value of GAPDH. Differences in the amount of target genes were then compared among the treatment groups.

Western blot analysis to detect changes in pathway factor protein levels. Cells washed with PBS were lysed using RIPA lysis buffer for 30 min on ice, and then the cells were collected and resuspended until the solution was as clear as possible. The supernatant was centrifuged at 4˚C, 13,400 x g, for 10 min, and subsequently, the protein concentration was calculated using a BCA kit (cat. no. E-BC-K318-M; Elabscience Biotechnology, Inc.) to calculate protein concentration. Proteins were diluted with saline to adjust the concentration of each sample, then mixed with 5X SDS sample buffer in a 4:1 ratio and denatured at 95˚C for 10 min. The protein samples were separated by electrophoresis on a 10% SDS gel (cat. no. G2043; Wuhan Servicebio Technology Co., Ltd.) by SDS-PAGE, and subsequently transferred to a PVDF membrane (cat. no. IPVH00010l; MilliporeSigma). The membranes were blocked with 5% skimmed milk powder (cat. no. GC310001; Wuhan Servicebio Technology Co., Ltd) or 5% bovine serum albumin [used explicitly for phosphorylated (p-) protein blocking, cat. no. GC305010; Wuhan Servicebio Technology Co., Ltd.] at room temperature for 1.5 h. Next, the membranes were incubated with anti-Salusin-α rabbit polyclonal antibodies (1:1,000; cat. no. ab232928; Abcam), anti-AMPK-α rabbit polyclonal antibodies (1:1,000; cat. no. AF6423; Affinity Biosciences), anti-phospho-AMPK-α (Thr172) rabbit polyclonal antibodies (1:1,000; cat. no. AF3423; Affinity Biosciences), anti-LKB1 rabbit polyclonal antibodies (1:500; cat.no. A2122; ABclonal Technology), anti-p-LKB1(Ser 428) rabbit polyclonal antibodies (1:1,000; cat. no. AP0602; ABclonal Biotech Co., Ltd.), antiSREBP1 rabbit polyclonal antibodies (1:1,000; cat. no. ab28481, Abcam), anti-FASN rabbit polyclonal antibodies (1:1,000; cat. no. FNab03019; Wuhan Fine Biotech Co., Ltd.), or anti-GAPDH rabbit monoclonal antibodies (1:10,000; cat. no. ab181602; Abcam) at 4˚C overnight. After washing the membranes with TBST (containing 0.1% Tween 20) they were incubated on a shaker with horseradish peroxidase (HRP)-labeled goat anti-rabbit

Table I. Sequences of primers used for semi-quantitative PCR.

Gene name	Primer sequence (5'→3')	Length (bp)
Salusin-α	F: CA**GGATCC**AGTGGTGCCCTTCCTCCCG	101
	R: CAT**CTCGAG**CTTGGCTCCAGGCCCAGC	
GAPDH	F: GTCTCCTCTGACTTCAACAGCG	131
	R: ACCACCCTGTTGCTGTAGCCAA	
MCP-1	F: CAGCCAGATGCAATCAATGCC	190
	R: TGGAATCCTGAACCCACTTCT	
TGF-β	F: CTAATGGTGGAAACCCACAACG	209
	R: TATCGCCAGGAATTGTTGCTG	
AMPK	F: TCCGAGGAAATCAAGGCACC	297
	R: GCCAAGCTGGCTGGTTACTA	
LKB1	F: CATGACTGTGGTGCCGTACT	140
	R: CATTGTGACTGGCCTCCTCT	
SREBP-1c	F: CACCGTTTCTTCGTGGATGG	116
	R: GTCACACAGTTCAGTGCTCGCTC	
ACC	F: TGGTAATGCGGTATGGAAGTCG	309
	R: TGTATGTTGTCCCTAAGGATTGTGC	
FASN	F: CAAATTCGACCTTTCTCAGAACCAC	293
	R: CCCCCTTCAACACTGCCTCC	

The text highlighted in bold represents the restriction site. MCP-1, monocyte chemoattractant protein-1; AMPK, adenosine 5'-monophosphate (AMP)-activated protein kinase; LKB1, liver kinase B1; SREBP-1c, sterol regulatory element binding protein-1c; ACC, acetyl-CoA carboxylase; FASN, fatty acid synthase F, forward; R, reverse.

IgG antibodies [1:10,000; cat. no. E-AB-1102; Elabscience Biotechnology, Inc.)] for 40 min. Subsequently, the membrane was treated with an ECL Ultra-sensitive Chemiluminescence kit (cat. no. MA0186; Dalian Meilun Biology Technology Co., Ltd.) and visualized using a chemiluminescence imaging system. The grayscale values of each group's target proteins and reference proteins were calculated using ImageJ for densitometric analysis.

Inhibitor induction. Dorsomorphin (Compound C, 10 μM; cat. no. GC17243; GLPBIO), an inhibitor of AMPK (20), was used to treat cells alongside transfection with the lentiviral vectors. Cells were inoculated in two six-well plates at a density of $1x10^6$ cells/well for 24 h until they reached 70% density, and cells in one plate were transfected with the virus following, as aforementioned. By contrast, cells in the other plate were co-treated with the inhibitor in addition to the virus. After 24 h, 200 μM FFA was added to all wells except for the control group. After a further 24 h of culturing, the cells were examined as aforementioned.

Statistical analysis. Statistical analysis was performed using GraphPad Prism version 9.5 (GraphPad Software, Inc.; Dotmatics) and SPSS version 26.0 (IBM Corp), and data are presented as the mean ± SD of three repeats. First, a normality test was performed. When the variances were homogeneous, A paired Student's t-test was used to compare differences between any two groups and one-way analysis of variance (ANOVA) followed by Tukey's multiple comparisons test was used to compare multiple sets of data. When the variances were not homogeneous, a Kruskal-Wallis H rank sum test was used to compare differences between multiple groups. All tests were two-tailed, and $P<0.05$ was considered to indicate a statistically significant difference.

Results

Successful establishment of the cell steatosis model. All the cells in the antibiotic-only group died after 3 days, and the average titer of the virus was finally obtained as $0.86x10^6$ IFU/ml after counting the number of viable cells in the control and antibiotic-treated groups. The optimal Multiplicity of infection (MOI) of HepG2 was determined to be 10 in a previous study (18); based on the average titer of the virus and the MOI, the amount of viral fluid added per well was calculated to be 1 ml. TEM images confirmed that lentiviral particles could be observed in the pHAGE-Salusin-α and pLKO.1-shSalusin-α groups, while no viral particles were observed in the control group, indicating successful lentiviral packaging (Fig. 1A). SQ-PCR was used to determine the expression of Salusin-α mRNA in HepG2 cells transfected with the overexpression or interference Salusin-α vectors. pHAGE group was significantly different from pHAGE-Salusin-α group and shMock group was significantly different from shSalusin-α group ($P<0.001$). And compared with the control group, the expression of Salusin-α in the overexpression group increased, while in the interference group, it decreased ($P<0.001$), indicating successful transfection of the virus (Fig. 1B and C). Moreover,

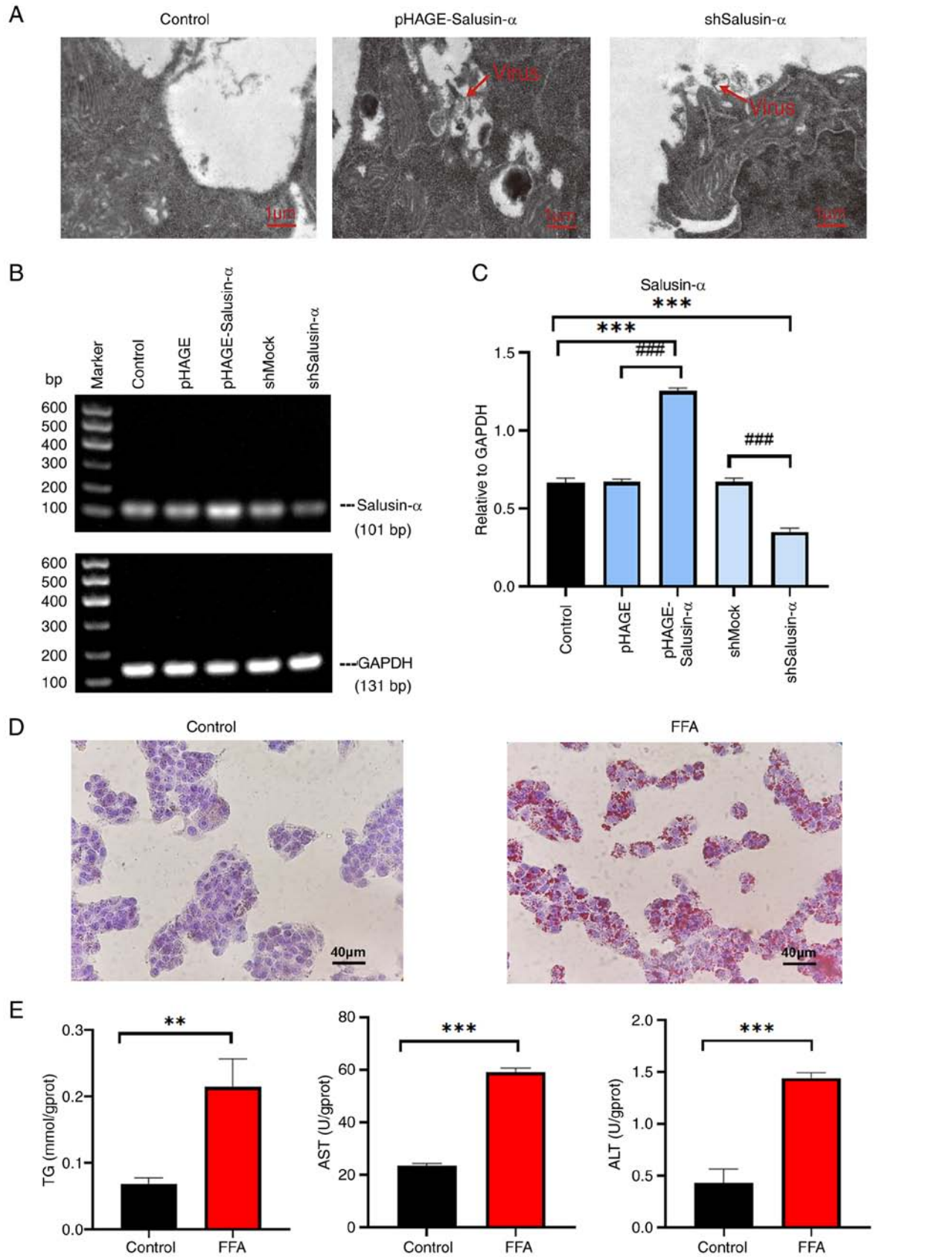

Figure 1. Construction of the lentivirus and establishment of the cell steatosis model. (A) Transmission electron microscopy of 293T cells in the control, pHAGE-Salusin-α and shSalusin-α groups 72 h after plasmid transfection. Red arrows indicate lentiviral particles. No viral particles were observed in the Control group. Scale bar, 1 μm. (B) Electrophoresis result graphs of the viral fluids of each group following RNA extraction, reverse transcription and PCR. The size of the Salusin-α sequence was 101 bp. (C) The results were analyzed using semi-quantitative PCR, and the relative expression of Salusin-α was indicated by comparing the ratio of Salusin-α/GAPDH. (D) Oil red O-stained cytogram of the Control and FFA groups. Scale bar, 40 μm. (E) Levels of TG, AST and ALT in the HepG2 cells in each group. Data are presented as the mean ± SD of three independent repeats. **P<0.01 and ***P<0.001 vs. control; $^{###}$P<0.001 vs. pHAGE or shMock. shRNA, short hairpin RNA; pHAGESalusinα, Salusinα overexpression; TEM, transmission electron microscopy, FFA, free fatty acids; TG, triglyceride; AST, aspartate aminotransferase; ALT, alanine aminotransferase; sh-, short hairpin; ns, not significant.

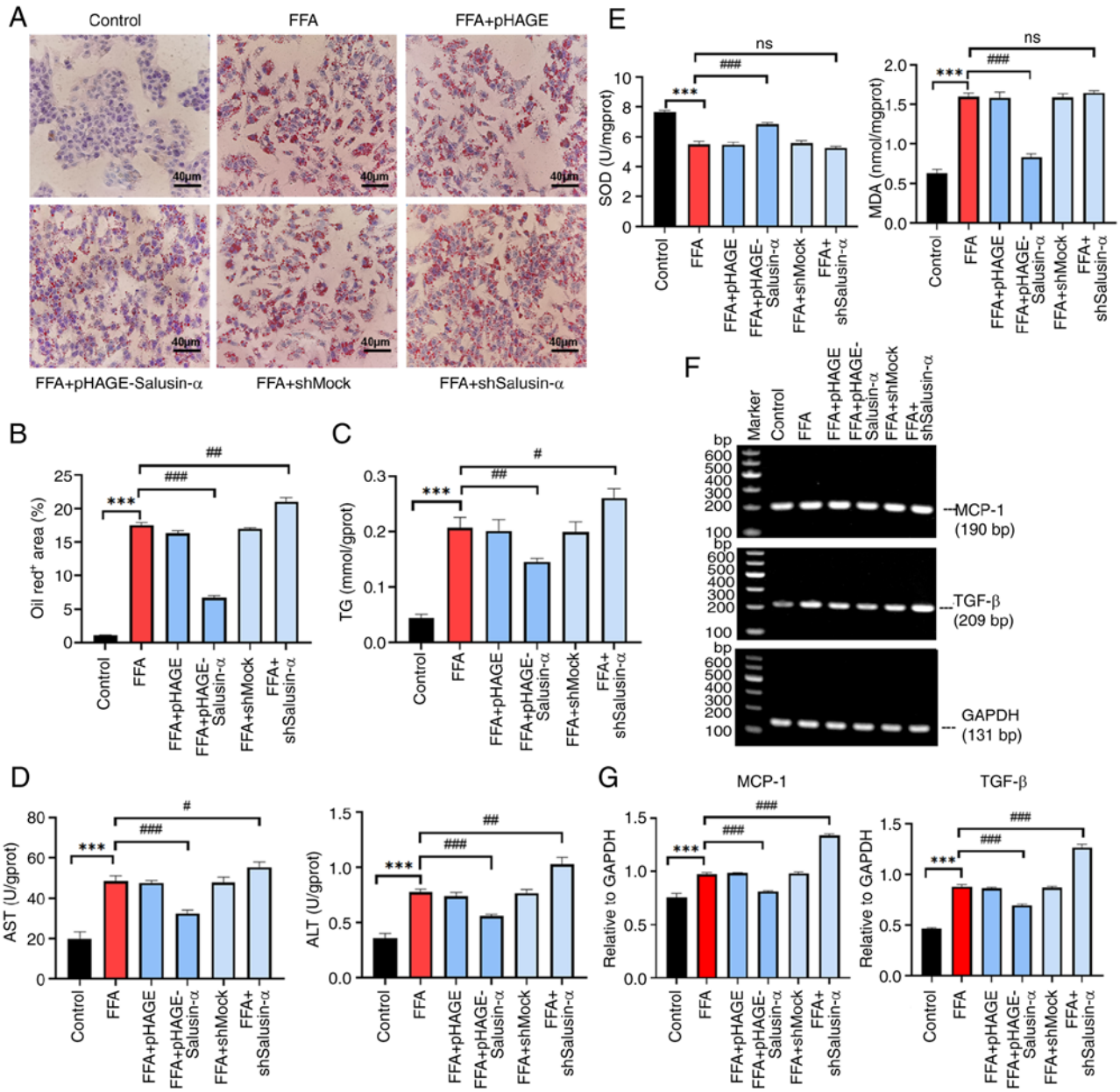

Figure 2. Effects of overexpression and knockdown of Salusin-α on lipid accumulation, oxidative stress, and inflammation. (A) Oil red O-stained cell maps of the control group, FFA group, FFA + pHAGE group, FFA + pHAGE-Salusin-α group, FFA + shMock group and FFA + shSalusin-α group. Scale bar, 40 μm. (B) Quantification of lipid content in the oil red O-stained cells by calculating the intracellular lipid droplet area. (C and D) Intracellular (C) TG and (D) AST and ALT levels were detected using biochemical kits. (E) Determination of the expression levels of SOD and MDA in HepG2 cells. (F) Graphs showing the electrophoretic results of PCR analysis of the inflammatory factors MCP-1 and TGF-β as well as GAPDH with sequence sizes of 190, 209, and 131 bp. (G) Results were analyzed using semi-quantitative PCR relative to GAPDH. Data are presented as the mean ± SD of three independent repeats. ***P<0.001 vs. Control; $^{\#}$P<0.05, $^{\#\#}$P<0.01 and $^{\#\#\#}$P<0.001 vs. FFA group. FFA, free fatty acids; TG, triglyceride; AST, aspartate aminotransferase; ALT, alanine aminotransferase SOD, superoxide dismutase, MDA, malondialdehyde; MCP-1, monocyte chemoattractant protein-1; TGF-β, transforming growth factor-β; sh-, short hairpin; ns, not significant.

the protein content of Salusin-α detected after transfection also showed significant differences between the overexpression and knockdown groups compared with the corresponding viral vectors (Fig. S1). Red lipid droplets were observed following oil red O staining in the FFA group (Fig. 1D), while the levels of TG, ALT and AST in the FFA group were all increased (Fig. 1E) (P<0.01). The results indicated that the fatty model of hepatocytes was successfully constructed.

Overexpression of Salusin-α alleviates lipid accumulation, oxidative stress and inflammation in HepG2 cells, while knockdown of Salusin-α has the opposite effect. To observe whether Salusin-α could reduce FFA-induced lipid accumulation in HepG2 cells, oil red O staining was used to assess the degree of lipid accumulation. The results of oil red O staining following the different treatments are shown in Fig. 2A. The lipid content in the FFA group was significantly increased compared with that of the control group (P<0.001), and the lipid content in the overexpression Salusin-α group was significantly lower than that of the FFA group, whereas the staining in the Salusin-α knockdown group was the largest (Fig. 2B; P<0.01). The

Table II. Specific values for each biochemical index.

Group	Index				
	TG (mmol/gprot)	ALT (U/gprot)	AST (U/gprot)	SOD (U/mgprot)	MDA (nmol/mgprot)
control	0.04±0.01	0.36±0.04	19.81±3.41	7.66±0.09	0.63±0.05
FFA	0.21±0.02	0.78±0.02[a]	48.42±2.69[a]	5.48±0.22[a]	1.60±0.05[a]
FFA + pHAGE	0.20±0.02	0.74±0.04	47.57±1.19	5.45±0.19	1.58±0.04
FFA + pHAGE-Salusin-α	0.16±0.01[c]	0.56±0.02[d]	32.27±1.74[d]	6.84±0.11[d]	0.83±0.04[d]
FFA + shMock	0.20±0.02	0.77±0.03	47.86±2.57	5.56±0.20	1.59±0.05
FFA + shSalusin-α	0.26±0.02[b]	1.03±0.06[c]	55.25±2.62[b]	5.24±0.10	1.65±0.03

The units of TG, ALT, AST, SOD and MDA are respectively mmol/gprot, U/gprot, U/gprot, U/mgprot and nmol/mgprot. The aforementioned experiments were performed three times independently, and the results were displayed as the mean ± SD. [a]P<0.001 vs. control; [b]P<0.05, [c]P<0.01 and [d]P<0.001 vs. FFA group. FFA, free fatty acid; TG, triglycerides; ALT, alanine aminotransferase; AST, aspartate aminotransferase; SOD, superoxide dismutase; MDA, malondialdehyde; sh-, short hairpin.

levels of TG, AST and ALT in the FFA group increased significantly compared with that in the control group; in the Salusin-α overexpression group, the levels decreased to varying degrees compared with the FFA group, and in the Salusin-α knockdown group, they increased to different degrees (Fig. 2C and D).

The excess inflammatory response caused by NAFLD also induces oxidative stress in cells, further damaging liver cells. To further explore whether Salusin-α could delay or reduce the extent of this damage, the levels of SOD and MDA in the cells were determined. The MDA levels in the FFA group were higher than that of the control group, whereas the SOD levels were lower (P<0.001). Following overexpression of Salusin-α, the levels of MDA decreased, whereas those of SOD increased (Fig. 2E). The specific values of these biochemical indicators are shown in Table II. SQ-PCR was used to detect the mRNA expression levels of MCP-1 and TGF-β. It was also found that the levels of these inflammatory factors in the FFA group were higher than that in the control group (P<0.001), and the levels of these two inflammatory factors in the Salusin-α overexpression group were reduced compared with that in the FFA group. By contrast, the levels in the knockdown group were significantly increased (P<0.001) (Fig. 2F and G). These results suggested that the overexpression of Salusin-α can help to alleviate the inflammatory damage response caused by the disorder of lipid metabolism, and the effect is opposite after knockdown.

Bioinformatics analysis shows that the LKB1/AMPK pathway is involved in lipid metabolism. Given that Salusin-α may play a crucial role in the lipid metabolism pathway in NAFLD, bioinformatics analysis was performed using data on patients with NAFLD obtained from GEO. The volcano map demonstrated that there were 85 upregulated genes and 7 downregulated genes in 72 patients with severe NAFLD compared with normal as well as patients with mild NAFLD (Fig. 3A). GO enrichment analysis showed that a series of changes such as inflammation, vascular development, cell migration and immune response occurred during steatosis with regard to biological processes, cellular component and molecular function (Fig. 3B). The GO enrichment analysis of DEGs revealed that NAFLD activated genes associated with the 'TGF-β signaling' pathway. In addition, 11.7% of the genes were involved in the PI3K-Akt and LKB1-AMPK signaling pathway (Fig. 3C). Pre-experiments on both pathway genes and the SQ-PCR results revealed that the LKB1 levels in the FFA + pHAGE-Salusin-α group were higher than that in the FFA group, while in the FFA + shSalusin-α group, the levels were reduced. At the same time, it was found that there was no significant difference in the change of PI3K content (data not shown), thus the LKB1/AMPK pathway was chosen to continue the experiment (Fig. 3D).

Overexpression and knockdown of Salusin-α regulates lipid degeneration in HepG2 cells via the LKB1/AMPK pathway. To determine whether Salusin-α exerted an inhibitory effect on lipid accumulation in HepG2 cells via the LKB1/AMPK signaling pathway, the mRNA expression levels of LKB1, AMPK, SREBP-1c, ACC and FASN (all of which are members of this pathway), as well as the protein expression levels of p-LKB1, LKB1, p-AMPK, AMPK, SREBP1 and FASN, were assessed. In the FFA + pHAGE-Salusin-α group, the expression of LKB1 and AMPK was slightly higher than that in the FFA group, whereas in the FFA + shSalusin-α group, the levels were reduced. SREBP-1c, FASN and ACC expression in the FFA + pHAGE-Salusin-α group was reduced. By contrast, in the FFA + shSalusin-α group, their expression levels were increased (Fig. 4A). This indicated that the levels of LKB1 and AMPK in the FFA + pHAGE-Salusin-α group increased slightly compared with the FFA group and were closer to those in the control group; and SREBP-1c, ACC, as well as FASN expression levels, were reduced. By contrast, the FFA + shSalusin-α group exhibited more pronounced changes, aligning with the observed trend in the FFA group (Fig. 4B-F).

The levels of each protein were altered following transfection (Fig. 5A-E). The levels of p-LKB1 and p-AMPK in the FFA group were lower than those in the Control group, and the

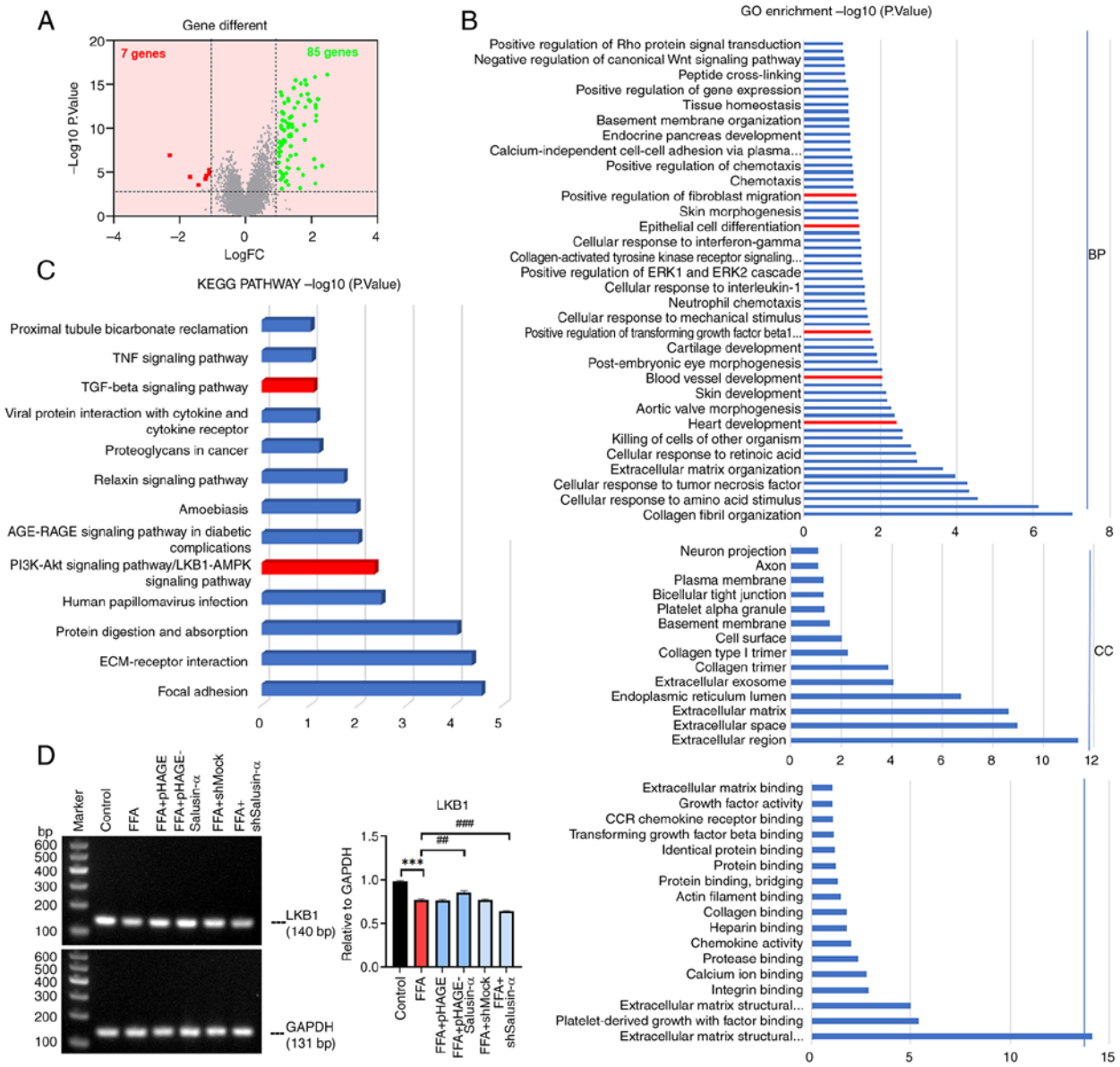

Figure 3. Bioinformatics analysis. (A) Volcano plots (log_2-fold change) were used to show the upregulated and downregulated genes in patients with severe NAFLD compared with normal and mild patients. (B) GO enriched terms associated with the DEGs in patients with NAFLD. (C) KEGG enriched pathways related to DEGs in patients with NAFLD. (D) Relative expression of LKB1 in different groups. Data are presented as the mean ± SD. ***P<0.001 vs. Control; $^{\#\#}$P<0.01 and $^{\#\#\#}$P<0.001 vs. FFA group. NAFLD, non-alcoholic fatty liver disease; GO, Gene Ontology; KEGG, Kyoto Encyclopedia of Genes and Genomes; DEG, differentially expressed gene; LKB1, liver kinase B1; FFA, free fatty acid; sh-, short hairpin.

levels in the FFA + shSalusin-α group were lower than those in the FFA group. The SREBP1 and FASN levels were higher in the FFA + shSalusin-α group compared with the FFA group. By contrast, in the FFA + pHAGE-Salusin-α group, they were lower (Fig. 5F). After transfecting cells with the Salusin-α overexpression plasmids and then stimulating cells with FFA, it was found that the phosphorylation levels of LKB1 and AMPK increased to a certain extent. The levels of SREBP1 and FASN decreased (P<0.01) compared with those of the FFA group, and after knockdown of Salusin-α, the protein levels of p-LKB1 and p-AMPK decreased, whereas the levels of SREBP1 and FASN were significantly increased (Fig. 5G-J; P<0.001). Therefore, it could be preliminarily determined that Salusin-α regulated the LKB1/AMPK pathway and may thus play a role in alleviating lipid metabolism disorders through this signaling pathway.

Inhibition of AMPK further indicates that Salusin-α overexpression and knockdown regulate the LKB1/AMPK pathway. Compound C, an AMPK inhibitor, was used to treat cells alongside the transfection experiments to evaluate the alterations in the downstream-related molecules. According to the proportion of lipid area to cell area, the addition of the inhibitor to the FFA group resulted in more notable changes to fat and an increase in lipid area. Following overexpression of Salusin-α and treatment with Compound C, the lipid droplet area was larger than that of the group treated with Salusin-α overexpression alone. This suggested that AMPK was inhibited, and Salusin-α was unable to exert the effect of alleviating lipid accumulation through the AMPK pathway. Additionally, the lipid droplet area was significantly increased following interference of Salusin-α co-treated with Compound C (Fig. 6A and B).

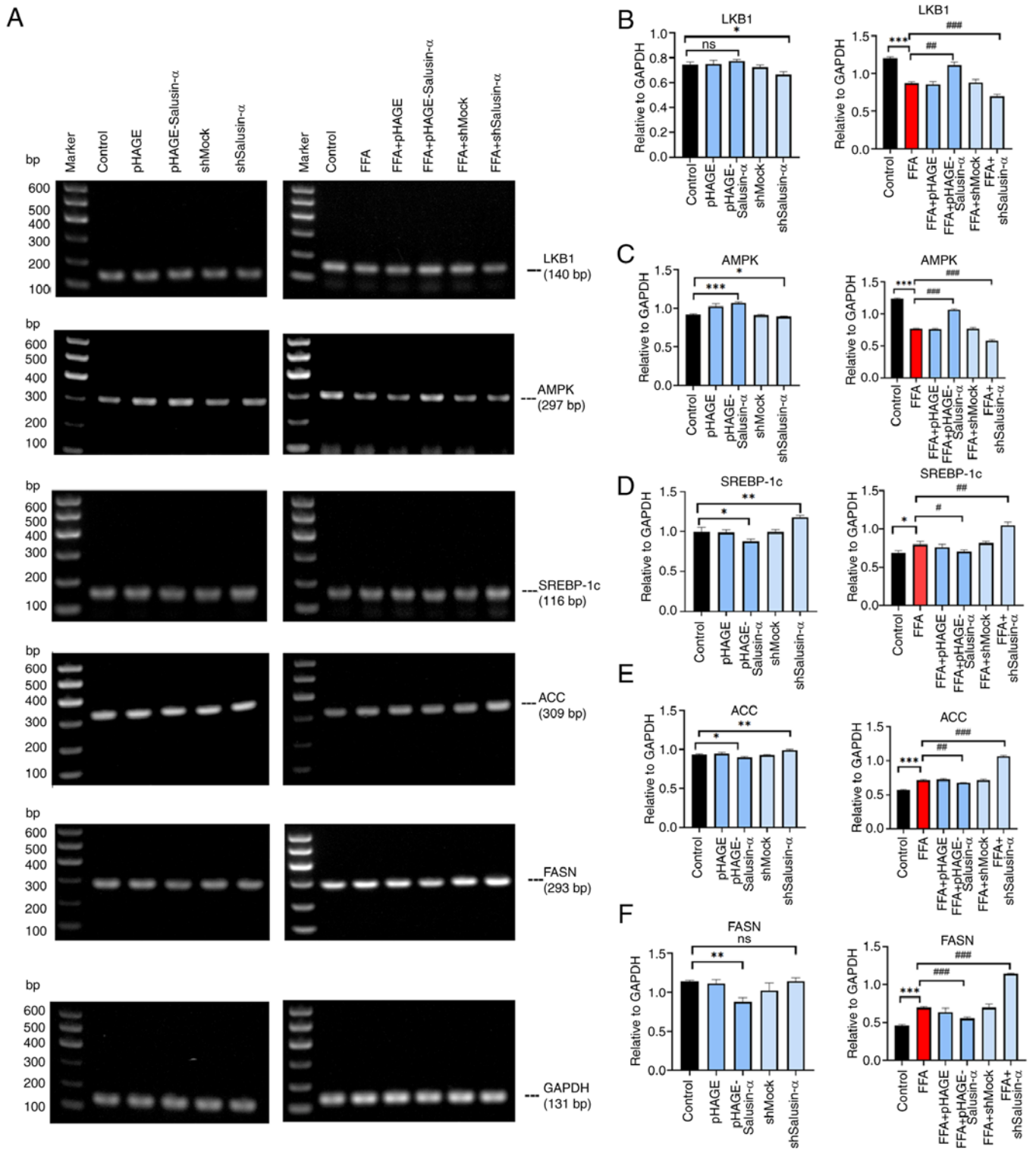

Figure 4. Effects of overexpression and knockdown of Salusin-α on downstream molecules. (A) LKB1, AMPK, SREBP-1c, ACC and FASN PCR electrophoresis results. The first column shows the molecular changes of each group after transfecting virus for 24 h. The second column shows the molecular changes after 24 h of virus transfection followed by 24 h of FFA induction. (B-F) Relative expression of (B) LKB1, (C) AMPK, (D) SREBP-1c, (E) ACC and (F) FASN in the different groups. Data are presented as the mean ± SD. *P<0.05, **P<0.01 and ***P<0.001 vs. control; $^{\#}$P<0.05, $^{\#\#}$P<0.01 and $^{\#\#\#}$P<0.001 vs. FFA group. LKB1, liver kinase B1; AMPK, adenosine 5'-monophosphate (AMP)-activated protein kinase; SREBP-1c, sterol regulatory element binding protein-1c; ACC, acetyl-CoA carboxylase; FASN, fatty acid synthase; FFA, free fatty acid; sh-, short hairpin; ns, not significant.

The mRNA expression levels of LKB1 and AMPK in the FFA + pHAGE-Salusin-α + Compound C group were lower than those in the FFA + pHAGE-Salusin-α. The mRNA expression levels of SREBP-1c, FASN and ACC in the FFA + shSalusin-α + Compound C group were higher than those in the FFA + shSalusin-α group (Fig. 7A). The mRNA expression levels of SREBP-1c, ACC and FASN content in the FFA group were higher than that of the control group (P<0.001).

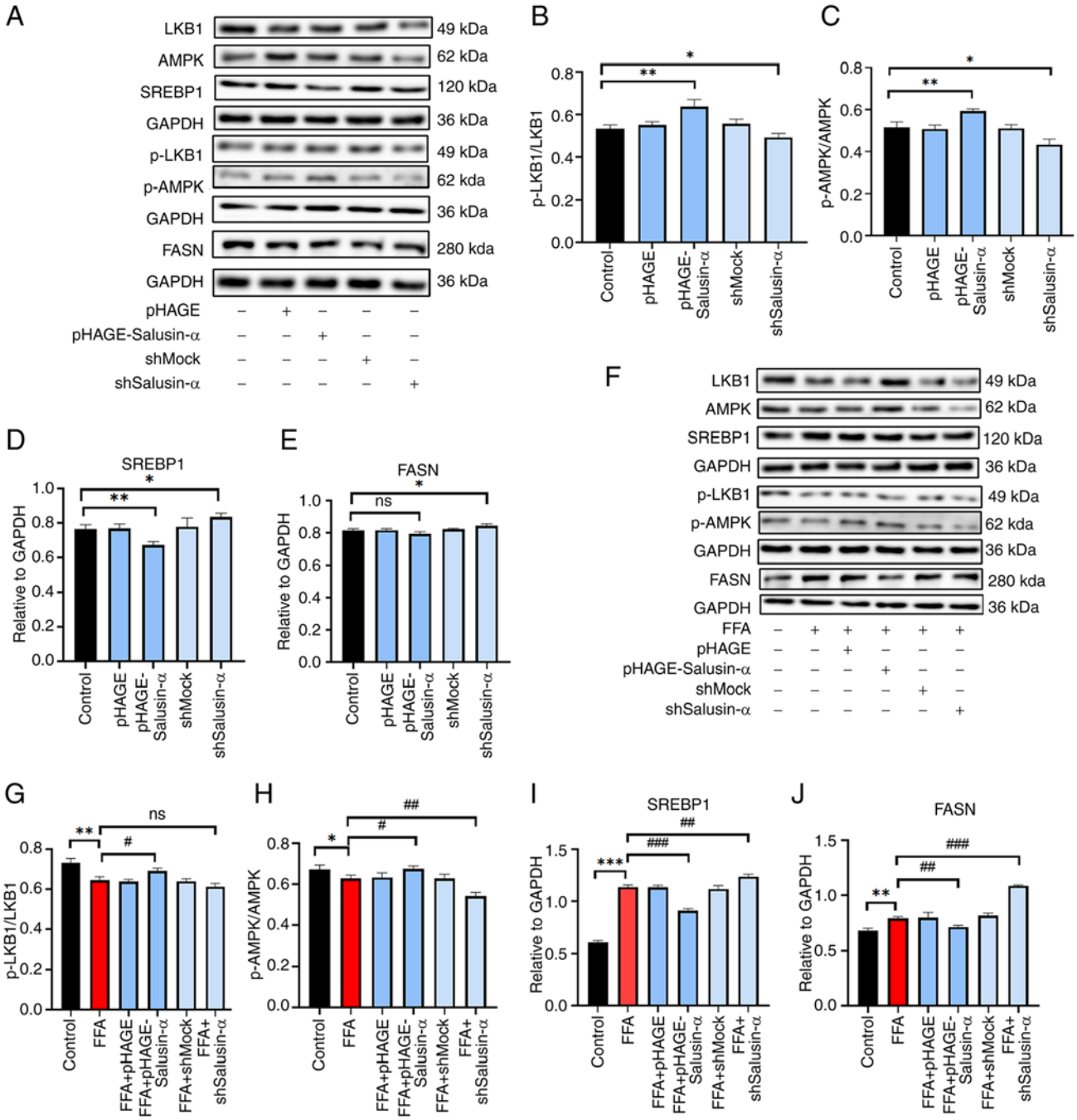

Figure 5. Validation of Salusin-α regulation of lipid metabolism via the LKB1/AMPK pathway by western blotting. (A) After lentiviral transfection of HepG2 cells for 24 h, western blotting was used to detect the expression of several proteins in the LKB1/AMPK downstream pathway. Expression of (B) p-LKB1/LKB1, (C) p-AMPK/AMPK, (D) SREBP-1c and (E) FASN in each group. (F) Lentiviruses were transfected for 24 h and then cells were induced with FFA for 24 h. The bar graphs show the densitometric analysis of the western blots. (G-J) Expression of (G) p-LKB1/LKB1, (H) p-AMPK/AMPK, (I) SREBP-1c and (J) FASN in the different treatment groups. Data are presented as the mean ± SD. *P<0.05, **P<0.01 and ***P<0.001 vs. control; $^{\#}$P<0.05, $^{\#\#}$P<0.01 and $^{\#\#\#}$P<0.001 vs. FFA group. LKB1, liver kinase B1; AMPK, adenosine 5'-monophosphate (AMP)-activated protein kinase; SREBP-1c, sterol regulatory element binding protein-1c; FASN, fatty acid synthase; p-, phosphorylated; FFA, free fatty acid; sh-, short hairpin; ns, not significant.

The addition of compound C further exacerbated this upregulation. In addition, compound C further decreased AMPK expression but had little effect on LKB1 levels (P>0.05). The mRNA levels of SREBP-1c, FASN and ACC in the Salusin-α overexpression group were lower than those in the FFA group. The addition of Compound C partially reversed the modulatory effect of Salusin-α. By contrast, the mRNA expression levels of SREBP-1c, ACC and FASN were the highest after co-treatment of Salusin-α knockdown and Compound C (Fig. 7B-F).

The protein expression levels of p-AMPK in the FFA + Compound C group were lower than those of the FFA group, and the expression levels of FFA + pHAG E-Salusin-α + Compound C group were slightly lower than those of the FFA + pHAGE-Salusin-α group, which reduced the phosphorylation level of AMPK. By contrast, the levels of p-LKB1 did not exhibit notable changes in the different groups. The levels of SREBP1 and FASN were higher in the FFA + shSalusin-α + Compound C group

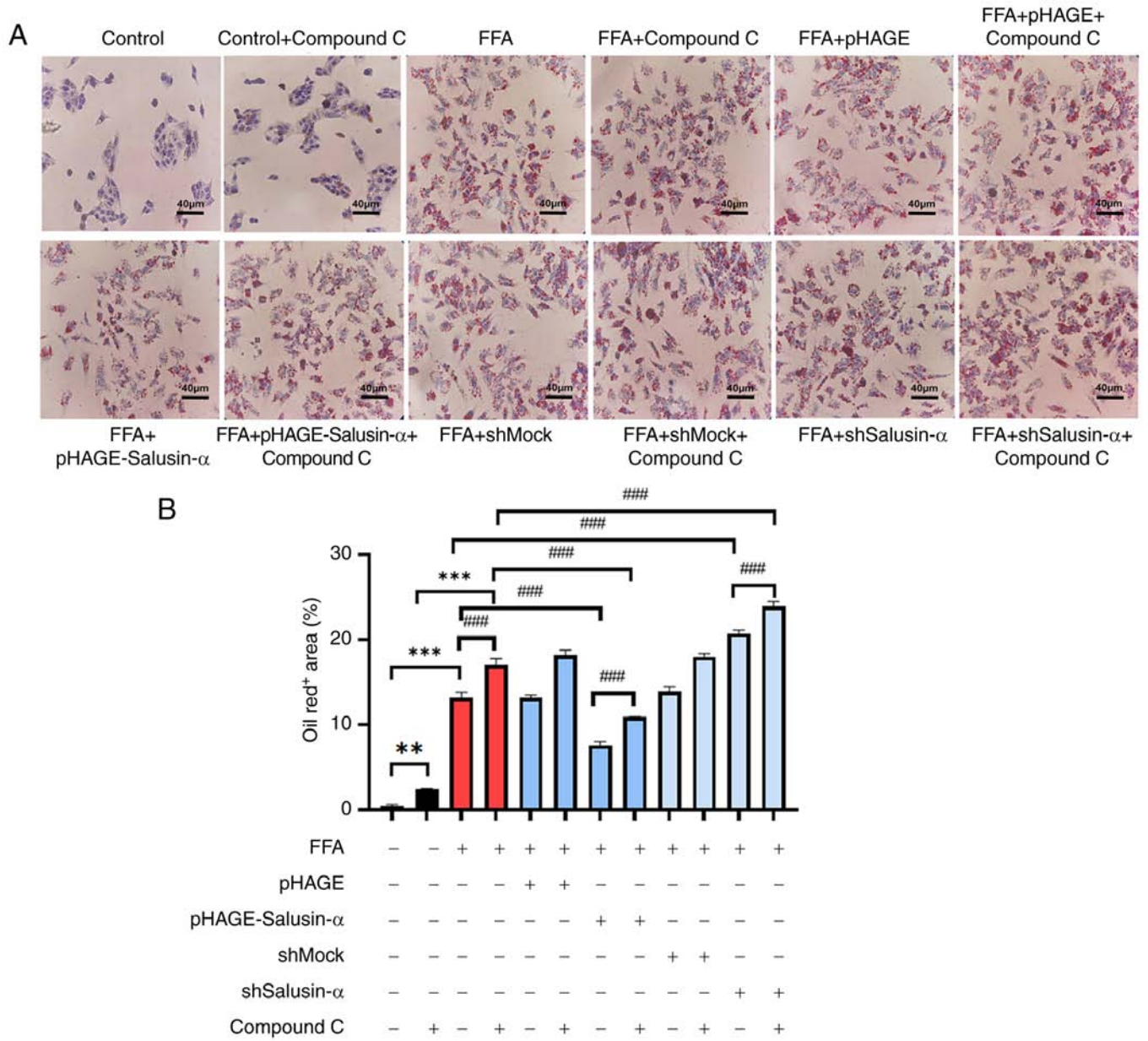

Figure 6. Treatment with an AMPK inhibitor increased the degree of lipid accumulation. (A) Oil red O staining of cells in the control group, control + compound C group, FFA group, FFA + compound C group, FFA + pHAGE group, FFA + pHAGE + compound C group, FFA + pHAGE-Salusin-α group, FFA + pHAGE-Salusin-α + Compound C group, FFA + shMock group, FFA + shMock + compound C group, FFA + shSalusin-α group and FFA + shSalusin-α + compound C group. Scale bar, 40 μm. (B) Quantification of lipid content in oil red O-stained cell. Data are presented as the mean ± SD of three repeats. **P<0.001 and ***P<0.001 vs. control; $^{###}$P<0.001 vs. FFA group. AMPK, adenosine 5'-monophosphate (AMP)-activated protein kinase; FFA, free fatty acid; sh, short hairpin; ns, not significant.

than in the FFA + shSalusin-α group, and the expression levels in the FFA + Compound C group were significantly higher than that in the FFA group (Fig. 8A). Compound C treatment further reduced the p-AMPK/AMPK ratio in the Salusin-α overexpressing cells, while it had little effect on the p-LKB1/LKB1 ratio. Additionally, the SREBP1 and FASN protein expression levels in both the Salusin-α overexpression and knockdown groups were increased after the addition of the inhibitor compared with the same treatment without the inhibitor (Fig. 8B-E), thus demonstrating that the inhibitory effect of Salusin-α on lipid droplets in FFA-treated HepG2 cells was partially attenuated when treated with an AMPK inhibitor.

Discussion

Previous studies have shown that both Salusin-α and -β are important cardiovascular regulatory peptides and may have opposite effects on lipid metabolism; and there are relatively few studies on the direction of lipid metabolism of Salusin-β, which needs further confirmation. The authors' research group previously found that overexpression of Salusin-β would decrease the expression of AdipoR1 and thus increase lipid accumulation (19). Salusin-α may serve as a therapeutic target for the management of atherosclerosis, hypertension and other coronary artery diseases by reducing lipid accumulation, reducing vascular endothelial inflammation, and reducing

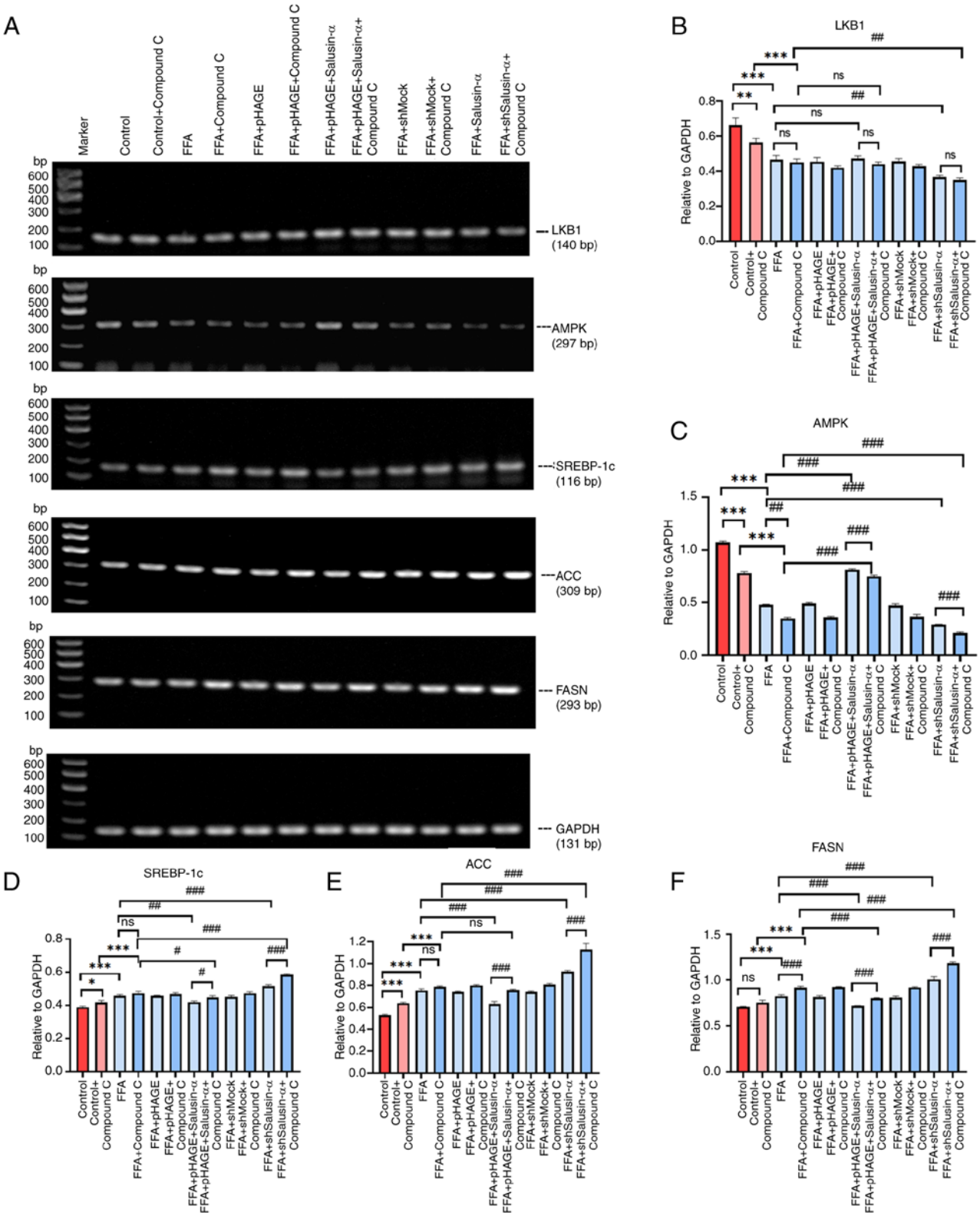

Figure 7. PCR was used to confirm the molecular changes following treatment with the inhibitors. (A) Images of agarose gels following PCR amplification of LKB1, AMPK, SREBP-1c, ACC, FASN and GAPDH in each group. (B-F) Relative expression of (B) LKB1, (C) AMPK, (D) SREBP-1c, (E) ACC and (F) FASN. Data are presented as the mean ± SD. *P<0.05, **P<0.01 and ***P<0.001 vs. control; $^{\#}$P<0.05, $^{\#\#}$P<0.01 and $^{\#\#\#}$P<0.001 vs. FFA group. LKB1, liver kinase B1; AMPK, adenosine 5'-monophosphate (AMP)-activated protein kinase; SREBP-1c, sterol regulatory element binding protein-1c; ACC, acetyl-CoA carboxylase; FASN, fatty acid synthase; FFA, free fatty acid; sh, short hairpin; ns, not significant.

foam cell formation (13-15,21). Disorders of lipid metabolism are the causes of these aforementioned diseases. In the case of abnormal lipid levels, hyperlipidemia eventually progresses to chronic vascular diseases such as atherosclerosis, and can also induce the development and/or progression of a series of metabolic diseases such as NAFLD (22,23). Since Salusin-α

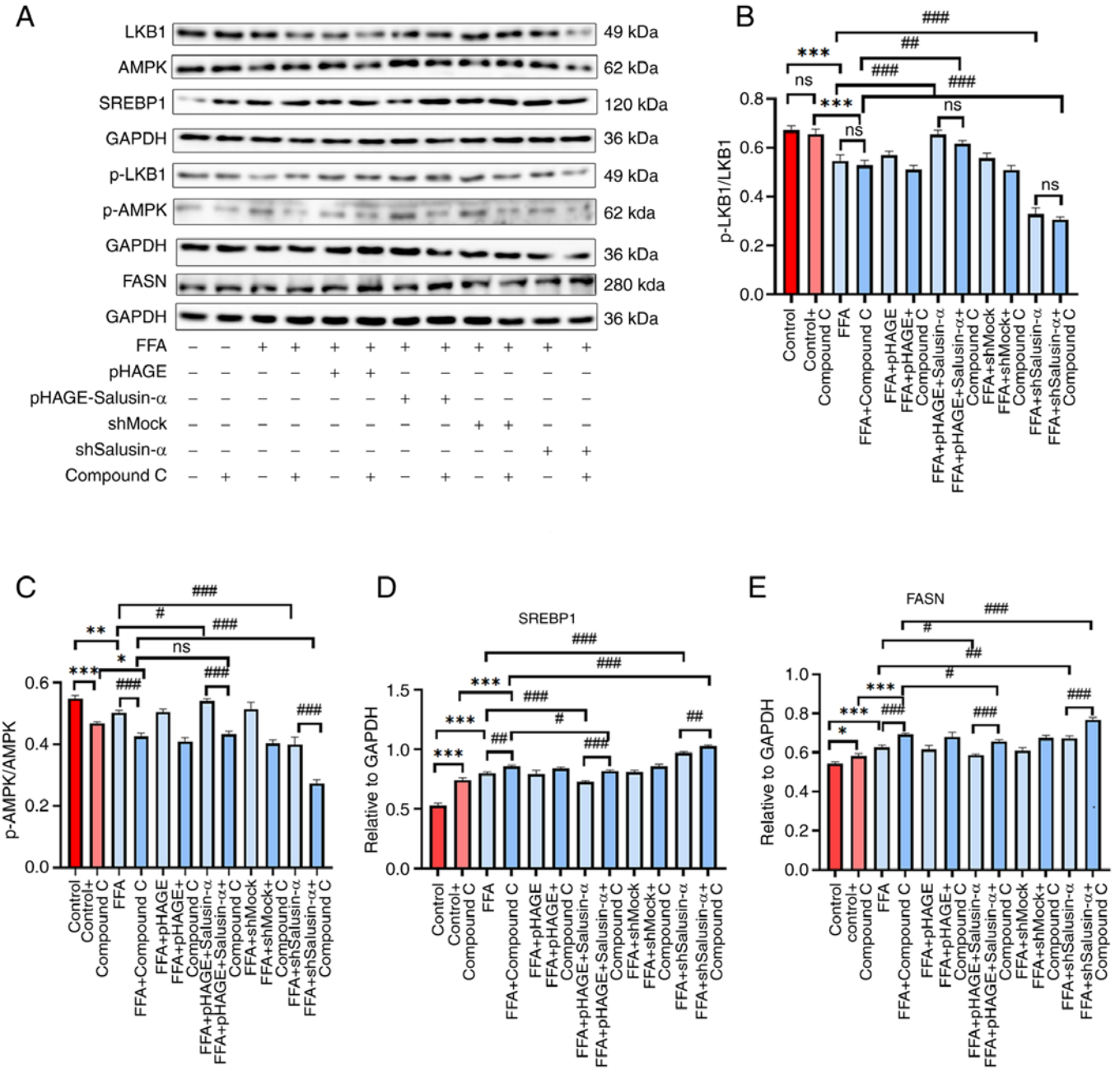

Figure 8. Western blotting was used to confirm the changes in the expression of downstream molecules following addition of inhibitors. (A) The induction of FFA in HepG2 cells after 24 h transfection with the lentivirus and Compound C was compared with that after transfection with the virus alone, and western blotting was used to detect the expression of each protein downstream in the LKB1/AMPK pathway. (B-E) Protein expression levels of (B) p-LKB1/LKB1, (C) p-AMPK/AMPK, (D) SREBP-1c and (E) FASN in each group. Data are presented as the mean ± SD. *P<0.05, **P<0.01 and ***P<0.001 vs. control; $^{\#}$P<0.05, $^{\#\#}$P<0.01 and $^{\#\#\#}$P<0.001 vs. FFA group. FFA, free fatty acid; LKB1, liver kinase B1; AMPK, adenosine 5'-monophosphate (AMP)-activated protein kinase; p-, phosphorylated; SREBP-1c, sterol regulatory element binding protein-1c; FASN, fatty acid synthase; sh, short hairpin; ns, not significant.

regulates lipid metabolism, it is possible that it also plays a vital role in NAFLD. It has been previously shown in animal experiments that Salusin-α can inhibit liver steatosis in mice and reduce plasma TG levels (16); however, the exact mechanism of its influence on lipid metabolism in hepatocytes remains unclear. The present study demonstrated for the first time, to the best of our knowledge, the specific mechanism by which Salusin-α alleviates lipid metabolism disorders in HepG2 cells. Salusin-α was identified to regulate the LKB1/AMPK pathway, thus providing a potential target for the prevention of NAFLD. In future studies, the interference of other diseases shall be also excluded and a lipid metabolism disorder model will be constructed in animals to further verify this conclusion.

Unlike previous experiments involving protein injections into animals, the lentiviral vectors used in the present study were effectively integrated into the chromosomes of HepG2 cells as previously described (18), holding the advantage of long-lasting lentiviral infection and stable expression of the target gene over an extended period of time, that is maintained throughout cell division and thus subsequent generations (24). In addition, the selection of cells as experimental objects, compared

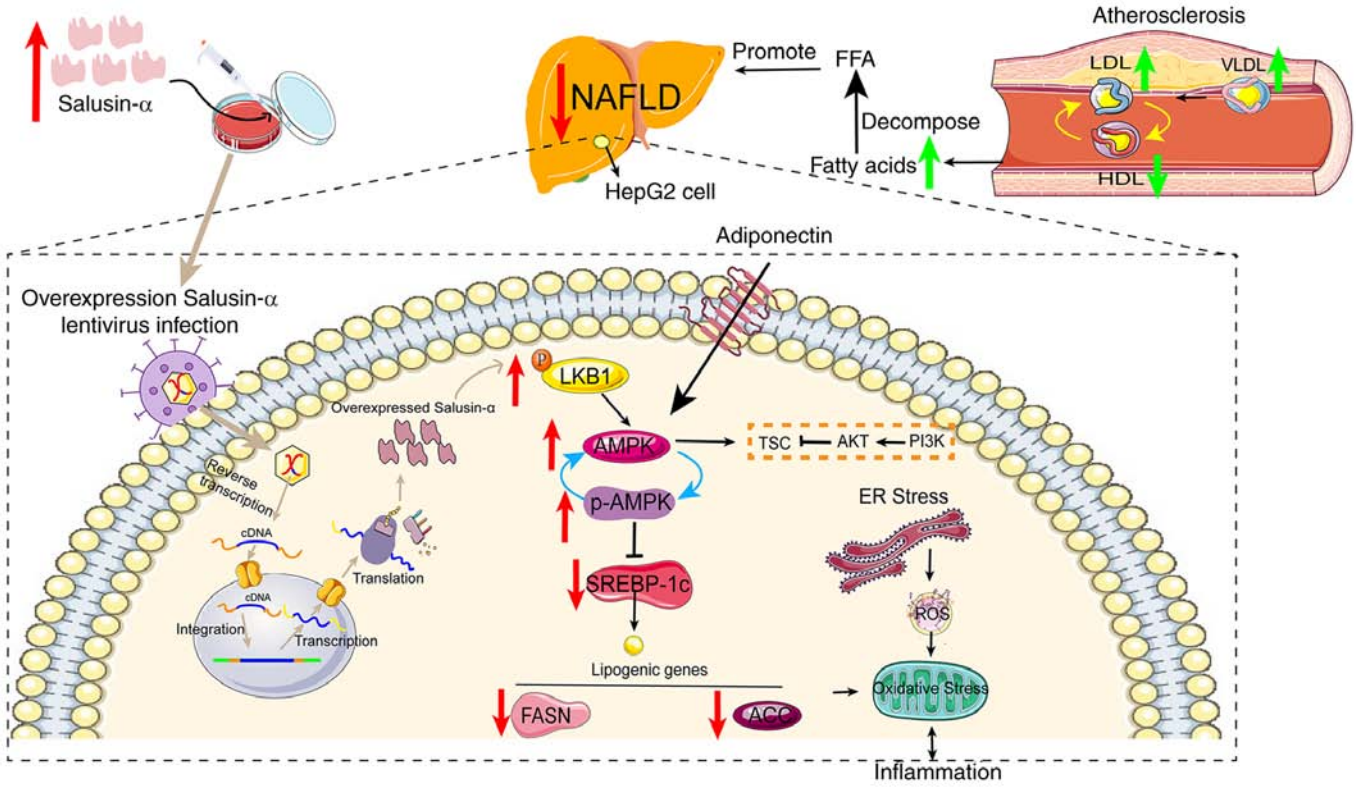

Figure 9. Hypothesized molecular mechanism depicting how Salusin-α ameliorates lipid metabolism disorders via regulation of the LKB1/AMPK signaling pathway. Salusinα was overexpresses or knocked down using lentiviruses. Salusin-α upregulated LKB1 expression and thus activated AMPK, which resulted in a decrease in the downstream SREBP-1c/FASN/ACC levels, thus reducing the severity of NAFLD. AS and NAFLD are causative factors in the deterioration of the other respective disease, and the elevated levels of LDLs in blood vessels leads to an increase in fatty acid content and worsens the degree of NAFLD. Gray arrows indicate the mechanistic process by which lentiviral vectors transport and regulate Salusin-α expression. Red arrows indicate changes in the expression of signaling pathway molecules following overexpression of Salusin-α in HepG2 cells, and green arrows indicate the changes in intravascular lipoprotein during the development of AS. LKB1, liver kinase B1; AMPK, adenosine 5'-monophosphate (AMP)-activated protein kinase; NAFLD, non-alcoholic fatty liver disease; FASN, fatty acid synthase; ACC, acetyl-CoA carboxylase; AS, atherosclerosis; LDL, low density lipoprotein; VLDL, very low-density lipoprotein; HDL, high-density lipoprotein; ROS, reactive oxygen species; SREBP-1c, sterol regulatory element binding protein-1c; ER, endoplasmic reticulum; p-, phosphorylated.

with the direct animal experiments, has certain advantages: The cost is lower, the time is shorter, the verification can be repeated several times, and the additional damage to the animals due to the immature technology can be avoided to a certain extent. To induce adipogenesis, FFAs were used, which are the simplest form of lipids found in adipose tissue and are essential in energy storage and cell signaling *in vivo* (25). The results showed that FFA, as an inducer, could mimic the *in vivo* environment and facilitate the differentiation of hepatocytes into adipocytes, reflecting the physiological process of cellular steatosis in an improved way.

Thus, HepG2 cells were transfected with lentiviral vectors for Salusin-a overexpression or knockdown, and then different groups of cells were induced by FFA. The changes in the various lipid metabolism indices before and after transfection and induction were observed. It was found that the expression of molecules related to lipid metabolism began to change after viral injection into cells. In particular, following FFA induction, the lipid drop area of the overexpression Salusin-α group was smaller than that of the FFA group, and the levels of TG, ALT and AST were reduced, while the lipid accumulation in the interference Salusin-α group was higher than that in the FFA group, suggesting that Salusin-α inhibited lipid production, promoted lipid oxidation, and prevented lipid accumulation. Additionally, it was observed that after FFA-induced cell lipidation, the levels of the inflammatory factors MCP-1 and TGF-β in cells increased, which again confirmed that abnormal lipid metabolism could induce inflammation. This is because imbalances in lipid metabolism produce reactive oxygen species (ROS) that over-oxidize lipids (26), and excess lipid accumulation not only leads to dyslipidemia but also endoplasmic reticulum stress (27), resulting in increased levels of pro-inflammatory cytokines, thus triggering a series of reactions associated with liver injury (3,28). The continuous inflammatory response further causes excessive ROS accumulation and thus oxidative stress, which leads to degeneration and necrosis of hepatocytes and ultimately, the production of MDA, a peroxidized end-product (29,30). In contrast to MDA, SOD is a major member of the antioxidant system and is used to protect cell structure and function from oxidative damage. Therefore, assessing the levels of both can reflect the degree of oxidative stress in the body and indirectly reflect the degree of liver cell damage and fibrosis. It was found that following overexpression of Salusin-α, the levels of markers of oxidative stress (MDA and SOD) respectively decreased and increased compared with the FFA group, while interference with Salusin-a demonstrated the opposite results. These results suggested that Salusin-α can mitigate inflammation and

oxidative stress in hepatocytes by regulating lipid metabolism. It is hypothesized that Salusin-α may serve as a biomarker for the early prevention and detection of lipid metabolism disorders (31).

To further elucidate the underlying mechanism by which Salusin-α alleviated disordered lipid metabolism in hepatocytes in the *in vitro* model of NAFLD, bioinformatics analysis was performed on the exome of 72 fatty liver disease samples in a dataset obtained from GEO to identify differentially expressed genes that were upregulated and downregulated in patients with NAFLD to determine the signaling pathways related to lipid metabolism in hepatocytes. The results highlighted two key signaling pathways; the PI3K-Akt (32) and LKB1-AMPK, closely related to hepatic lipid metabolism. Pre-experiments on these two pathways were performed, which indicated that Salusin-α appeared to have a stronger impact on LKB1 and AMPK compared with PI3K and AKT, as determined by SQ-PCR. Moreover, previous studies have also confirmed that the LKB1/AMPK pathway is a key pathway regulating lipid metabolism and is closely related to energy metabolism, and may thus serve as a therapeutic target for NAFLD (33,34). There are few studies on the mechanism of Salusin-α to alleviate lipid metabolism disorder (16,18). Thus, it is worth investigating whether the mechanism underlying the improvements in lipid metabolism exerted by Salusin-α involves the LKB1/AMPK pathway in hepatocytes.

Given that Salusin-α may exert an inhibitory effect on lipid accumulation in HepG2 cells through the LKB1/AMPK signaling pathway, the mRNA expression levels of LKB1, AMPK, SREBP-1c, ACC and FASN (all members of the pathway), as well as the protein expression levels of p-LKB1, LKB1, p-AMPK, AMPK, SREBP1 and FASN were determined. AMPK, a crucial regulator of metabolism and mitochondrial homeostasis, could be activated through LKB1, which is a key upstream kinase, whereas SREBPs, of which there are three isoforms in mammalian cells (SREBP-1a, -1c, and -2), are major regulators of lipid metabolism that regulate lipid oxidation and catabolism (35). Additionally, SREBP-1c, which primarily governs the synthesis of fatty acids, can be activated by AMPK at the serine (Ser)372 site, leading to the inhibition of the translocation of SREBP-1c into the nucleus, thus regulating TG synthesis (36-38). ACC and FASN are downstream substrates of SREBP-1c and serve as crucial enzymes in regulating hepatic TG metabolism (39). Notably, the present study showed that following the overexpression of Salusin-α in HepG2 cells and stimulation with FFA, the expression levels of LKB1 and AMPK were increased compared with that in the FFA group, while the expression of SREBP-1c, ACC and FASN decreased; the opposite results were observed following Salusin-α knockdown. Thus, it was preliminarily confirmed that overexpression of Salusin-α activated AMPK by promoting LKB1 phosphorylation, which in turn downregulated the expression levels of SREBP-1c, and decreased the expression of its target genes FASN and ACC, thereby inhibiting the synthesis of TG, cholesterol and fatty acids, accelerating the oxidative decomposition of fatty acids, reducing the deposition of lipids in the liver, and ultimately ameliorating hepatic steatosis (40).

To further confirm that the changes in the levels of SREBP-1c, FASN and ACC were caused by the changes in the levels of AMPK following the alterations to Salusin-α expression, compound C, an inhibitor of AMPK, was also added in subsequent experiments. It was found that lipid accumulation in the compound C-treated group was higher than that in the non-compound C-treated group, indicating that the inhibition of AMPK in cells could not degrade lipids through this pathway. It is worth noting that although the levels of cellular adipose in the FFA + pHAGE-Salusin-α + compo und C group were lower than that in the FFA + compound group, it was higher than that in the FFA + pHAGE-Salusin-α group. Moreover, the levels of cellular adipose in the FFA + shSalusin-α + Compound C group were higher than that in the FFA + compound C group. These results suggested that Salusin-α content has an important effect on the severity of lipidation in HepG2 cells, but its inhibitory effect on lipid accumulation in hepatocytes was limited by AMPK inhibitors. Correspondingly, following compound C treatment, the expression of AMPK decreased, and the expression levels of the downstream molecules SREBP-1c, FASN and ACC increased, resulting in intracellular lipid accumulation; however, the levels of the LKB1, an upstream molecule, were not affected by the inhibitor. These findings revealed that Salusin-α regulated lipid metabolism through the LKB1/AMPK/SREBP-1c signaling pathway. Salusin-α-mediated alleviation of lipid metabolism disorders is a complex process, and whether Salusin-α acts directly or indirectly on key molecules in the pathway through other molecules is unclear. These questions remain to be answered in future studies. Therefore, the next key step is to conduct *in vivo* studies of the role of Salusin-α to further validate the experimental conclusions after excluding other disease factors that interfere with the lipid metabolism disorder model.

In conclusion, the results of the present study highlighted the potential of Salusin-α in reducing lipid accumulation and alleviating NAFLD via regulation of LKB1/AMPK phosphorylation (Fig. 9). Administration of FFA following Salusin-α overexpression accelerated lipolysis as well as fatty acid oxidation, and the extent of lipid accumulation was reduced, indicating that Salusin-α may play a role in the early prevention of NAFLD, also suggesting the importance of lipid metabolism *in vivo*. These results provide further insights into the role of Salusin-α in lipid metabolism and other cardiovascular aspects and provide potential targets for the prevention and treatment of NAFLD (41).

Acknowledgements

Not applicable.

Funding

The present study was supported by the Department of Higher Education, Ministry of Education, industry-university cooperative education project (grant no. 202002323015).

Availability of data and materials

The data generated in the present study may be requested from the corresponding author.

Authors' contributions

JP and CY planned and performed experiments. JP wrote the main manuscript text. CY prepared figures. AX and HZ proposed the concept and design part of the experiment, and provided important suggestions during the writing of the manuscript. JP, YF, RZ and LC collected and analyzed the data. XL and YW analyzed and interpreted the data, contributed reagents or other essential material and reviewed and revised the content of the article. All authors read and approved the final manuscript. JP and CY confirm the authenticity of all the raw data.

Ethics approval and consent to participate

Not applicable.

Patient consent for publication

Not applicable.

Competing interests

The authors declare that they have no competing interests.

References

1. Chen M, Zhu J, Luo H, Mu W and Guo L: The journey towards physiology and pathology: Tracing the path of neuregulin 4. Genes Dis 11: 687-700, 2023.
2. Guo YY, Li BY, Xiao G, Liu Y, Guo L and Tang QQ: Cdo1 promotes PPARγ-mediated adipose tissue lipolysis in male mice. Nat Metab 4: 1352-1368, 2022.
3. Huang DQ, El-serag HB and Loomba R: Global epidemiology of NAFLD-related HCC: Trends, predictions, risk factors and prevention. J Nat Rev Gastroenterol Hepatol 18: 223-238, 2021.
4. Zhou F, Zhou J, Wang W, Zhang XJ, Ji YX, Zhang P, She ZG, Zhu L, Cai J and Li H: Unexpected rapid increase in the burden of NAFLD in China from 2008 to 2018: A systematic review and meta analysis. Hepatology 70: 1119-1133, 2019.
5. Powell EE, Wong VW and Rinella M: Non-alcoholic fatty liver disease. J Lancet 397: 2212-2224, 2021.
6. Wong VW, Adams LA, de Lédinghen V, Wong GL and Sookoian S: Noninvasive biomarkers in NAFLD and NASH-current progress and future promise. Nat Rev Gastroenterol Hepatol 15: 461-478, 2018.
7. Jin C, Zhou T, Duan Z, Deng Y, Zhang X, Xiao C, He J, He G, Zhou Y and Li S: Effect of chin brick tea [Camellia sinensis (L.) Kuntze] on lipid metabolism and inflammation by modulating intestinal flora and bile acids in mice with non-alcoholic fatty liver disease. J Ethnopharmacol 318: 116950, 2024.
8. Stefan N, Häring HU and Cusi K: Non-alcoholic fatty liver disease: Causes, diagnosis, cardiometabolic consequences, and treatment strategies. Lancet Diabetes Endocrinol 7: 313-324, 2019.
9. Shichiri M, Ishimaru S, Ota T, Nishikawa T, Isogai T and Hirata Y: Salusins: Newly identified bioactive peptides with hemodynamic and mitogenic activities. Nat Med 9: 1166-1172, 2003.
10. Nakayama C, Shichiri M, Sato K and Hirata Y: Expression of proSalusin in human neuroblastoma cells. Peptide 30: 1362-1367, 2009.
11. Nagashima M, Watanabe T, Shiraishi Y, Morita R, Terasaki M, Arita S, Hongo S, Sato K, Shichiri M, Miyazaki A and Hirano T: Chronic infusion of Salusin-alpha and -beta exerts opposite effects on atherosclerotic lesion development in apolipoprotein E-deficient mice. Atherosclerosis 212: 70-77, 2010.
12. Murphy SK, Yang H, Moylan CA, Pang H, Dellinger A, Abdelmalek MF, Garrett ME, Ashley-Koch A, Suzuki A, Tillmann HL, *et al*: Relationship between methylome and transcriptome in patients with nonalcoholic fatty liver disease. Gastroenterology 145: 1076-1087, 2013.
13. Chen M, Wang Z and Wang S: Research progress of Salusin-α in atherosclerotic cardiovascular disease. Chem Life 42: 326-331, 2022 (In Chinese).
14. Yang C and Yang J: Research progress on the role of salusins in the development of atherosclerosis. J Pract Med 30: 1663-1665, 2014 (In Chinese).
15. Niepolski L and Grzegorzewska AE: Salusins and adropin: New peptides potentially involved in lipid metabolism and atherosclerosis. Adv Med Sci 61: 282-287, 2016.
16. Tang K, Wang F, Zeng Y, Chen X and Xu X: Salusin-α attenuates hepatic steatosis and atherosclerosis in high fat diet-fed low density lipoprotein receptor deficient mice. Eur J Pharmacol 830: 76-86, 2018.
17. Wang Y, Luo M, Mao X, Shi X and Liu X: Targeted delivery of salusin-α into rabbit carotid arterial endothelium using SonoVue. J Ultrasound Med 41: 365-376, 2022.
18. Zhang H, Yan C, Wang S, Xu A, Zhang Q, Duan X, Gong G and Wang Y: Overexpression of Salusin-α upregulates AdipoR2 and activates the PPARα/ApoA5/SREBP-1c pathway to inhibit lipid synthesis in HepG2 cells. Int J Mol Med 51: 41, 2023.
19. Xu A, Wang L, Luo M, Zhang H, Ning M, Pan J, Duan X, Wang Y and Liu X: Overexpression of salusin-β downregulates adipoR1 expression to prevent fatty acid oxidation in HepG2 cells. Mol Med Rep 29: 18, 2024.
20. Kuang X, Lu F and Yi P: Effect of berberine on LKB1-AMPK-TORC2 signaling network in HepG2 insulin resistance cell model. Chin J Integr Chin West Med Dig 23: 467-471, 2015 (In Chinese).
21. Watanabe T, Nishio K, Kanome T, Matsuyama TA, Koba S, Sakai T, Sato K, Hongo S, Nose K, Ota H, *et al*: Impact of salusin-alpha and -beta on human macrophage foam cell formation and coronary atherosclerosis. Circulation 117: 638-648, 2008.
22. Zhang Y, Guo Z, Wang J, Yue Y, Yang Y, Wen Y, Luo Y and Zhang X: Qinlian hongqu decoction ameliorates hyperlipidemia via the IRE1-α/IKKB-β/NF-κb signaling pathway: Network pharmacology and experimental validation. J Ethnopharmacol 318: 116856, 2024.
23. Poznyak A, Grechko AV, Poggio P, Myasoedova VA, Alfieri V and Orekhov AN: The diabetes mellitus-atherosclerosis connection: The role of lipid and glucose metabolism and chronic inflammation. Int J Mol Sci 21: 1835, 2020.
24. Sweeney NP and Vink CA: The impact of lentiviral vector genome size and producer cell genomic to gag-pol mRNA ratios on packaging efficiency and titre. Mol Ther Methods Clin Dev 21: 574-584, 2021.
25. Yi J, Zhou Q, Huang J, Niu S, Ji G and Zheng T: Lipid metabolism disorder promotes the development of intervertebral disc degenerate. Biomed Pharmacother 166: 115401, 2023.
26. Zechner R, Zimmermann R, Eichmann TO, Kohlwein SD, Haemmerle G, Lass A and Madeo F: FAT SIGNALS-lipases and lipolysis in lipid metabolism and signaling. Cell Metab 15: 279-291, 2012.
27. Koh IU, Lim JH, Joe MK, Kim WH, Jung MH, Yoon JB and Song J: AdipoR2 is transcriptionally regulated by ER stress inducible ATF3 in HepG2 human hepatocyte cells. FEBS J 277: 2304-2317, 2010.
28. Li J, Wang S, Yao L, Ma P, Chen Z, Han TL, Yuan C, Zhang J, Jiang L, Liu L, *et al*: 6-gingerol ameliorates age-related hepatic steatosis: Association with regulating lipogenesis, fatty acid oxidation, oxidative stress and mitochondrial dysfunction. Toxicol Appl Pharmacol 362:125-135, 2019.
29. Xu N, Luo H, Li M, Wu J, Wu X, Chen L, Gan Y, Guan F, Li M, Su Z, *et al*: β-patchoulene improves lipid metabolism to alleviate non-alcoholic fatty liver disease via activating AMPK signaling pathway. Biomed Pharmacother 134: 111104, 2021.
30. Gong P, Long H, Guo Y, Wang Z, Yao W, Wang J, Yang W, Li N, Xie J and Chen F: Chinese herbal medicines: The modulator of nonalcoholic fatty liver disease targeting oxidative stress. J Ethnopharmacol 318: 116927, 2024.
31. Zhang J, Ma X and Fan D: Ginsenoside CK ameliorates hepatic lipid accumulation via activating the LKB1/AMPK pathway in vitro and in vivo. Food Funct 13: 1153-1167, 2022.
32. Li BY, Guo YY, Xiao G, Guo and Tang QQ: SERPINA3C ameliorates adipose tissue inflammation through the cathepsin G/Integrin/AKT pathway. Mol Metabol 61: 101500, 2022.
33. Saravia J, Raynor JL, Chapman NM, Lim SA and Chi H: Signaling networks in immunometabolism. Cell Res 30: 328-334, 2020.

34. Li Q, Tan JX, He Y, Bai F, Li SW, Hou YW, Ji LS, Gao YT, Zhang X, Zhou ZH, *et al*: Atractylenolide III ameliorates non-alcoholic fatty liver disease by activating hepatic adiponectin receptor 1-mediated AMPK pathway. Int J Biol Sci 18: 1594-1611, 2022.
35. Qiu B, Lawan A, Xirouchaki CE, Yi JS, Robert M, Zhang L, Brown W, Fernández-Hernando C, Yang X, Tiganis T and Bennett AM: MKP1 promotes nonalcoholic steatohepatitis by suppressing AMPK activity through LKB1 nuclear retention. Nat Commun 14: 5405, 2023.
36. Jang HJ, Lee YH, Dao T, Jo Y, Khim KW, Eom HJ, Lee JE, Song YJ, Choi SS, Park K, *et al*: Thrap3 promotes nonalcoholic fatty liver disease by suppressing AMPK-mediated autophagy. Exp Mol Med 55: 1720-1733, 2023.
37. Yin X, Liu Z and Wang J: Tetrahydropalmatine ameliorates hepatic steatosis in nonalcoholic fatty liver disease by switching lipid metabolism via AMPK-SREBP-1c-Sirt1 signaling axis. Phytomedicine 119: 155005, 2023.
38. Ruolan Z and Bo N: The pathogenesis and treatment progress of NAFLD targeted by SREBP-1 related path-way. J Progr Clin Med 12: 4210-4220, 2022.
39. Li C, Zhang L, Qiu Z, Deng W and Wang W: Key molecules of fatty acid metabolism in gastric cancer. Biomolecules 12: 706, 2022.
40. Zhang Z, Ye Z and Chen Y: Research progress on the role of AMPK signaling pathway in the development of nonalcoholic fatty liver disease. J Nanjing Med Univ (Nat Sci) 39: 1252-1256, 2019 (In Chinese).
41. Zhou CH, Pan J, Huang H, Zhu Y, Zhang M, Liu L and Wu Y: Salusin-β, but not salusin-α, promotes human umbilical vein endothelial cell inflammation via the p38 MAPK/JNK-NF-κB pathway. PLoS One 9: e107555, 2014.

Copyright © 2024 Pan et al. This work is licensed under a Creative Commons Attribution-NonCommercial-NoDerivatives 4.0 International (CC BY-NC-ND 4.0) License.